2007-10-15

The Drosophila homolog of MCPH1, a human microcephaly gene, is required for genomic stability in the early embryo

Jamie L. Rickmyre
Vanderbilt University Medical Center

Et al.

The *Drosophila* homolog of *MCPH1*, a human microcephaly gene, is required for genomic stability in the early embryo

Jamie L. Rickmyre[1], Shamik DasGupta[2], Danny Liang-Yee Ooi[3], Jessica Keel[1], Ethan Lee[1], Marc W. Kirschner[3], Scott Waddell[2] and Laura A. Lee[1,*]

[1]Department of Cell and Developmental Biology, Vanderbilt University Medical Center, U-4200 MRBIII, 465 21st Avenue South, Nashville, TN 37232-8240, USA
[2]Department of Neurobiology, University of Massachusetts Medical School, 364 Plantation Street, Worcester, MA 01605, USA
[3]Department of Systems Biology, Harvard Medical School, 200 Longwood Avenue, Boston, MA 02115, USA
*Author for correspondence (e-mail: laura.a.lee@vanderbilt.edu)

Accepted 20 August 2007
Journal of Cell Science 120, 3565-3577 Published by The Company of Biologists 2007
doi:10.1242/jcs.016626

Summary

Mutation of human microcephalin (*MCPH1*) causes autosomal recessive primary microcephaly, a developmental disorder characterized by reduced brain size. We identified *mcph1*, the *Drosophila* homolog of *MCPH1*, in a genetic screen for regulators of S-M cycles in the early embryo. Embryos of null *mcph1* female flies undergo mitotic arrest with barrel-shaped spindles lacking centrosomes. Mutation of Chk2 suppresses these defects, indicating that they occur secondary to a previously described Chk2-mediated response to mitotic entry with unreplicated or damaged DNA. *mcph1* embryos exhibit genomic instability as evidenced by frequent chromatin bridging in anaphase. In contrast to studies of human *MCPH1*, the ATR/Chk1-mediated DNA checkpoint is intact in *Drosophila mcph1* mutants. Components of this checkpoint, however, appear to cooperate with MCPH1 to regulate embryonic cell cycles in a manner independent of Cdk1 phosphorylation. We propose a model in which MCPH1 coordinates the S-M transition in fly embryos: in the absence of *mcph1*, premature chromosome condensation results in mitotic entry with unreplicated DNA, genomic instability, and Chk2-mediated mitotic arrest. Finally, brains of *mcph1* adult male flies have defects in mushroom body structure, suggesting an evolutionarily conserved role for MCPH1 in brain development.

Supplementary material available online at
http://jcs.biologists.org/cgi/content/full/120/20/3565/DC1

Key words: *Drosophila*, Embryogenesis, Microcephaly, Cell cycle, Mitosis, DNA checkpoint, BRCT domain

Introduction

Drosophila melanogaster is an ideal model organism for study of the cell cycle during development (reviewed by Foe et al., 1993; Lee and Orr-Weaver, 2003). *Drosophila* achieves rapid embryogenesis by using a streamlined cell cycle that is not dependent on transcription or growth. The first 13 embryonic cell cycles are nearly synchronous nuclear divisions without cytokinesis occurring in the shared cytoplasm of the syncytial blastoderm. These cycles differ from canonical G1-S-G2-M cycles in that they have no intervening gaps; instead DNA replication and mitosis rapidly oscillate. Maternal RNA and protein stockpiles drive these abbreviated 'S-M' cycles (~10 minutes each). In mammalian embryos, rapid peri-gastrulation divisions that occur later in development share many features and have been proposed to be related by evolutionary descent to early embryonic divisions of flies and frogs (O'Farrell et al., 2004). Thus, advances gained from studies of these streamlined cycles in 'simple' model organisms likely have relevance for understanding mammalian cell cycles.

In a genetic screen for regulators of embryonic S-M cycles, we identified the *Drosophila* homolog of a human disease gene, *MCPH1* (microcephalin). Mutation of human *MCPH1* causes autosomal recessive primary microcephaly, a developmental disorder characterized by severe reduction of cerebral cortex size (Jackson et al., 2002). *Mcph1* is highly expressed in the developing forebrain of fetal mice, consistent with its proposed role in regulating the number neuronal precursor cell divisions and, ultimately, brain size (Jackson et al., 2002). Human MCPH1 protein is predicted to contain three BRCA1 C-terminal (BRCT) domains (reviewed by Glover et al., 2004; Huyton et al., 2000), which mediate phosphorylation-dependent protein-protein interactions in cell-cycle checkpoint and DNA repair functions.

Several studies have implicated human MCPH1 in the cellular response to DNA damage. The DNA checkpoint is engaged at critical cell-cycle transitions in response to DNA damage or incomplete replication and serves as a mechanism to preserve genomic integrity (reviewed by Nyberg et al., 2002). Triggering of this checkpoint causes cell-cycle delay, presumably to allow time for correction of DNA defects. When a cell senses DNA damage or incomplete replication, a kinase cascade is activated. Activated ATM and ATR kinases phosphorylate their targets, including the checkpoint kinase Chk1, which is activated to phosphorylate its targets. The first clue that MCPH1 plays a role in the DNA damage response came from siRNA-mediated knockdown studies in cultured mammalian cells demonstrating a requirement for MCPH1 in the intra-S phase and G2-M checkpoints in response to ionizing

radiation (Lin et al., 2005; Xu et al., 2004). Two recent reports have further implicated MCPH1 in the DNA checkpoint, although puzzling discrepancies remain to be resolved (reviewed by Bartek, 2006). One report indicates that MCPH1 functions far downstream in the pathway, at a level between Chk1 and one of its targets, Cdc25 (Alderton et al., 2006). Another report (Rai et al., 2006) suggests that MCPH1 is a proximal component of the DNA damage response required for radiation-induced foci formation (i.e. recruitment of checkpoint and repair proteins to damaged chromatin).

Additional functions have been reported for MCPH1. *MCPH1*$^{-}$ lymphocytes of microcephalic patients exhibit premature chromosome condensation (PCC) characterized by an abnormally high percentage of cells in a prophase-like state, suggesting that MCPH1 regulates chromosome condensation and/or cell-cycle timing (Trimborn et al., 2004). A possible explanation for the PCC phenotype is that *MCPH1*-deficient cells have high Cdk1-cyclin B activity, which drives mitotic entry; decreased inhibitory phosphorylation of Cdk1 was found to be responsible for elevated Cdk1 activity in *MCPH1*-deficient cells (Alderton et al., 2006). It is not clear whether MCPH1's role in regulating mitotic entry in unperturbed cells is related to its checkpoint function; intriguingly, Chk1 has similarly been reported to regulate timing of mitosis during normal division (Kramer et al., 2004). *MCPH1* (also called *Brit1*) was independently identified in a screen for negative regulators of telomerase, suggesting that it may function as a tumor suppressor (Lin and Elledge, 2003). Further evidence for such a role comes from a study showing that gene copy number and expression of *MCPH1* is reduced in human breast cancer cell lines and epithelial tumors (Rai et al., 2006).

We report here the identification and phenotypic characterization of *Drosophila* mutants null for *mcph1*. We show that syncytial embryos from *mcph1* females exhibit genomic instability and undergo mitotic arrest due to activation of a DNA checkpoint kinase, Chk2. We find that, in contrast to reports of MCPH1 function in human cells, the ATR/Chk1-mediated DNA checkpoint is intact in *Drosophila mcph1* mutants. We propose that *Drosophila* MCPH1, like its human counterpart, is required for proper coordination of cell-cycle events; in early embryos lacking *mcph1*, chromosome condensation prior to completion of DNA replication causes genomic instability and Chk2-mediated mitotic arrest.

Results

Screen for *Drosophila* cell-cycle mutants identifies *absent without leave* (*awol*)

In an effort to identify genes required for S-M cycles of the early embryo, we previously screened (Lee et al., 2003) a maternal-effect lethal subset of a collection of ethylmethanesulfonate (EMS)-mutagenized lines from Charles Zuker's lab (Koundakjian et al., 2004). We screened ~2400 lines by examining DAPI-stained embryos of homozygous females. Because early embryonic development is entirely regulated by maternally deposited mRNA and protein, only the maternal genotype is relevant in this screen. We identified 33 lines (12 chromosome II and 21 chromosome III mutants) representing 26 complementation groups in which the majority of embryos from mutant females arrest at the syncytial blastoderm stage. We previously identified two alleles of *giant nuclei*, which prevents excessive DNA replication in S-M cycles (Freeman et al., 1986; Renault et al., 2003), from this collection (Lee et al., 2003). We have now identified alleles of four well-known regulators of the cell cycle from the same screen (supplementary material Table S1). All four genes encode protein kinases with conserved roles in cell-cycle regulation. *wee1*, *grapes*, *telomere fusion* and *aurora* encode *Drosophila* orthologs of Wee1 (a Cdk1 inhibitory kinase), DNA checkpoint kinases Chk1 and ATM (ataxia telangiectasia mutated), and the mitotic kinase Aurora A, respectively (Fogarty et al., 1997; Glover et al., 1995; Oikemus et al., 2004;

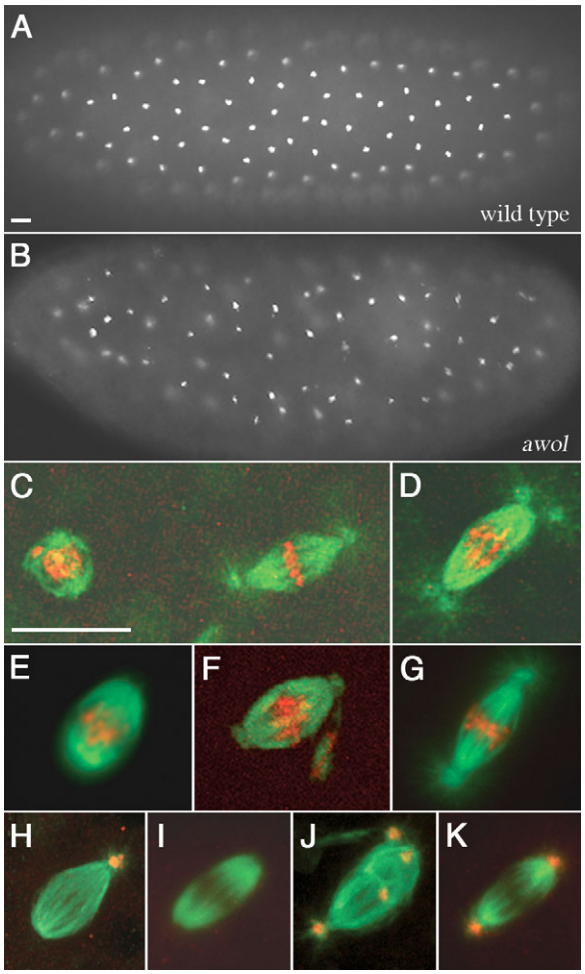

Fig. 1. The *awol* phenotype. Representative syncytial embryos (A,B) and mitotic spindles (C-K) in embryos from wild-type or *awol*^{Z1861}/*awol*^{Z0978} females. (A,B) DNA staining of embryos from *awol* females shows arrest with condensed chromosomes and unevenly spaced nuclei (B) compared to wild type (A). (C-G) Microtubules are in green and DNA in red. (C) Asynchronous neighboring nuclei in embryo from *awol* female (left, interphase; right, mitosis). (D) Metaphase spindle with duplicated centrosomes in embryo from *awol* female shows asynchronous nuclear and centrosome cycles (duplication normally occurs in telophase). (E) Shortened, barrel-shaped spindle in embryo from *awol* female. (F) DNA displaced from metaphase plate is tethered by microtubules to spindle pole in embryo from *awol* female. (G) Wild-type spindle. (H-K) Microtubules are in green and centrosomes in red. (H-I) *awol* spindles with missing or ectopic centrosomes. (K) Wild-type spindle. Bars, 20 μm.

Table 1. Mitotic spindle defects in *mcph1* embryos and suppression by *mnk*

Genotype	MI*	Centrosome number (% spindles)†		Other spindle defects (% spindles)†		
		Decreased‡	Increased§	Barrel	Interacting¶	Multipolar
Wild type	54.1	0.2	0.0	0.1	0.0	0.0
*mcph1***	88.8	43.6	46.0	97.5	0.0	0.2
mnk	54.2	0.2	0.1	0.0	0.2	0.0
mnk mcph1^{Z1861}	57.5	0.2	1.2	0.0	15.0	6.0

*Mitotic index=% embryos in mitosis/total number of embryos (>100 embryos scored per genotype). The presence of both condensed chromosomes and a mitotic spindle was used as the criterion for scoring mitotic embryos.
†To quantify spindle defects, >500 spindles from 25 embryos were scored per genotype.
‡Spindles with centrosomal detachment at one or both poles.
§Spindles with >1 centrosome per pole (one or both poles) or ectopic centrosomes within spindle. Telophase spindles were not scored because centrosome duplication normally occurs at this phase in the early embryo.
¶Two spindles connected by microtubules.
**$mcph1^{Z1861}/mcph1^{Z0978}$.

Price et al., 2000). Identification of these alleles of bona fide cell-cycle regulators validates our screen.

We chose for further study the largest complementation group on chromosome II (comprising *ZII-0978*, *ZII-1861* and *ZII-4050*) identified in our screen. Females homozygous or transheterozygous for any of these mutations are completely sterile, producing embryos that arrest in a metaphase-like state (~90% of embryos) in cycles 1-8 (the majority in cycles 6-8). Unevenly spaced, asynchronously dividing nuclei and centrosome duplication prior to chromosome segregation are often seen (Fig. 1B-D; Table 1); all of these are consistent with failure of nuclear divisions. Tubulin foci are frequently missing from one or both poles of mitotic spindles, which are typically shorter and more barrel-shaped than those of wild type (Fig. 1E; Table 1). Chromosomes are poorly aligned and occasionally displaced from the metaphase plate (Fig. 1F). Staining for Centrosomin, a core centrosomal component (Li and Kaufman, 1996), revealed that lack of tubulin foci at one or both poles in mutant-derived embryos is due to an absence of centrosomes (Fig. 1H,I; Table 1); we occasionally see ectopic centrosomes embedded in spindles (Fig. 1J; Table 1). On the basis of the phenotype of acentrosomal mitotic spindles, we have given the name '*absent without leave*' ('*awol*') to mutants of this complementation group.

awol encodes the *Drosophila* homolog of *MCPH1*

We localized *awol* to a region including five genes by a combination of mapping strategies (see Materials and Methods for details). A candidate in this region was the *Drosophila* homolog of the human disease gene, *MCPH1* (Jackson et al., 2002). Sequencing of PCR-amplified *mcph1* coding region from homozygous mutant genomic DNA revealed that $awol^{Z0978}$ and $awol^{Z4050}$ are distinct missense mutations in *mcph1* causing non-conservative amino acid changes and $awol^{Z1861}$ is a nonsense mutation resulting in severe truncation of the protein (Fig. 2A). Thus, all three EMS-induced *awol* alleles represent mutations affecting MCPH1 protein. Furthermore, females carrying any of these *awol* alleles in

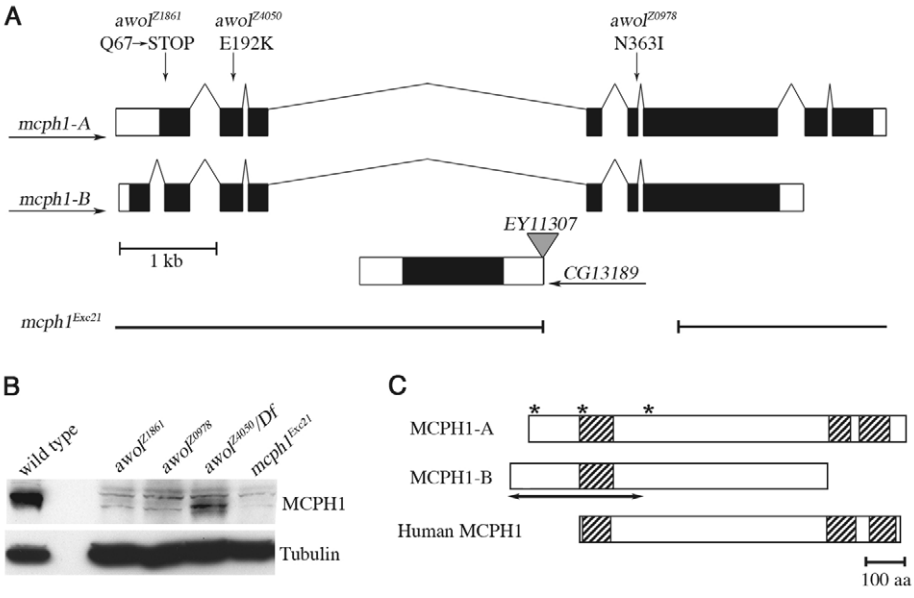

Fig. 2. *mcph1* is the *awol* gene. (A) The *Drosophila mcph1* gene structure. Exons are represented by filled boxes, 5′- and 3′-UTRs by open boxes, and splicing events by thin lines. The gene *CG13189* lies within the largest intron of *mcph1*. Alternative splicing produces transcript *mcph1-RA* or *-RB*. Arrows below gene or transcript names indicate direction of transcription. Positions of the point mutations in each of the three EMS-induced alleles of *awol* and resulting amino acid changes (numbers refer to MCPH1-B) are indicated above the *mcph1* gene. Imprecise excision of *P*-element *EY11307* (inverted triangle) generated allele $mcph1^{Exc21}$ (deleted region indicated by gap). (B) Western analysis reveals trace amounts of or no MCPH1 protein in extracts of *awol* embryos relative to wild type (loading control: anti-α-tubulin). The excision allele (*Exc21*) of *mcph1* serves as negative control. *Df=Df(2R)BSC39*, which removes the *mcph1* genomic locus. (C) Comparison of the BRCT domain content (hatched boxes) of the two *Drosophila* MCPH1 isoforms (MCPH1-A and -B) and human MCPH1 protein (bottom). Positions of the amino acid changes in each of the three EMS-induced alleles of *awol* are indicated by asterisks. A double-sided arrow indicates the region of MCPH1-B used for antibody production.

trans to a deletion of the *mcph1* genomic locus produce embryos with phenotypes indistinguishable from that of homozygous mutant females (data not shown), suggesting that all three Zuker *awol* alleles behave genetically as nulls.

To confirm that mutation of *mcph1* is responsible for the awol phenotype, we generated a null allele ($mcph1^{Exc21}$) by imprecise P-element excision (Fig. 2A). $mcph1^{Exc21}$ homozygous females produce embryos with the awol phenotype; similar results were obtained for females carrying this excision in *trans* to any of the EMS-induced *awol* alleles or a deletion of the *mcph1* genomic locus (data not shown), further confirming that mutation of *mcph1* causes the awol phenotype. Importantly, expression of transgenic *mcph1* using the UAS-Gal4 system (Brand and Perrimon, 1993; Rorth, 1998) restored fertility to $awol^{Z0978}/awol^{Z4050}$ females, resulting in a hatch rate of ~40% of their embryos (supplementary material Table S2). Thus, *mcph1* is the *awol* gene. We used the MCPH1 isoform that is most abundant in the early embryo for transgenic rescue; it is possible that full rescue of the maternal-effect lethality of *awol* mutants might additionally require expression of the less abundant isoform (see below for description of MCPH1 isoforms; Fig. 2A and supplementary material Fig. S1B).

To further characterize our *mcph1* alleles, we generated polyclonal antibodies against an MBP-MCPH1 fusion. Anti-MCPH1 antibodies recognize a major band of ~90 kDa, consistent with the predicted size of MCPH1-B, when used to probe immunoblots of wild-type embryo extracts (Fig. 2B). In contrast, for all *mcph1* alleles identified here, we detect greatly reduced or no MCPH1 protein in mutant-derived embryos. Thus, all of these alleles are null (or nearly null) for MCPH1 protein.

MCPH1 isoforms differ in expression pattern and BRCT domain content

Our genetic data revealed that *mcph1* null alleles are homozygous viable and that *mcph1* is required maternally for early embryonic development. To measure MCPH1 levels throughout *Drosophila* development, we probed immunoblots of extracts from various developmental stages with anti-MCPH1 antibodies (supplementary material Fig. S1A). As expected, MCPH1 is abundant in ovaries and early embryos, whereas older embryos under zygotic control have relatively low amounts. MCPH1 is present in larval brains and imaginal discs but undetectable in adult brain extracts. Although high levels of MCPH1 are present in adult testes, it is not required for male fertility (data not shown).

Two major isoforms of MCPH1 were detected by immunoblotting: ~90 kDa (predominant in ovaries and embryos) and ~110 kDa (predominant in testes). Both isoforms were detected in larval tissues. The most recent *mcph1* gene model annotated by FlyBase predicts two splice variants (A and B) differing at their 5′-ends that encode proteins with distinct amino termini (Grumbling and Strelets, 2006). We compared sizes of recombinant MCPH1-A and -B proteins (produced by in vitro transcription-translation reactions) to that of endogenous MCPH1 isoforms by immunoblotting. We found that the gel mobilities of MCPH1-A and -B closely match that of MCPH1 in testes and ovaries, respectively; thus, MCPH1-A is the ~110 kDa isoform that is abundant in testes, and MCPH1-B is the ~90 kDa isoform that is abundant in ovaries and early embryos (supplementary material Fig. S1B).

We observed a discrepancy between relative sizes of MCPH1-A and -B on our immunoblots (A larger than B; supplementary material Fig. S1B) and as predicted by FlyBase [779 versus 826 amino acids, respectively (Grumbling and Strelets, 2006)]. We were unable to find 3′-end sequence data for *mcph1-A* on public databases, so we fully sequenced a representative clone (LP15451) and found it to encode a protein of 981 amino acids, which closely matches our estimated size of 110 kDa for endogenous MCPH1-A. Furthermore, our sequencing revealed that *mcph1-A* contains coding sequence from both *mcph1* and *CG30038*, a gene predicted to overlap the 3′-end of *mcph1* (Fig. 2A). Thus, *mcph1-A* and *-B* are alternatively spliced at both ends, producing proteins that differ in their N- and C-terminal regions (Fig. 2C), and predicted gene *CG30038* comprises alternatively spliced exons of *mcph1-A*.

MCPH1-A and -B proteins both contain BRCT domains (three or one, respectively). The arrangement of BRCT domains within MCPH1-A (one N-terminal and two paired C-terminal) resembles that of human MCPH1 (Fig. 2C). *Drosophila* and human MCPH1 have highest sequence identity in their BRCT domains (37.6%, 52.5% and 26.8% between the N-terminal, first C-terminal, and second C-terminal domains, respectively). The presence of extended amino termini in both *Drosophila* isoforms relative to human MCPH1 raises the possibility that the reported human sequence (Jackson et al., 2002) may not be full-length.

MCPH1 is a nuclear protein

Because *Drosophila* MCPH1 contains BRCT domains, we hypothesized that it has a nuclear function. In syncytial embryos, MCPH1 signal localizes to interphase nuclei and disappears in mitosis (supplementary material Fig. S2). As control for antibody specificity, no MCPH1 signal was detected in interphase nuclei of embryos derived from *mcph1* null females. Because MCPH1 protein is readily detectable throughout the cell cycle (by immunoblotting of extracts from staged embryos; data not shown), the disappearance of MCPH1 signal in mitosis, as observed by immunostaining, is probably due to its dispersal into the cytoplasm upon nuclear envelope breakdown. Human MCPH1 has been reported to localize to the nucleus (Lin et al., 2005) as well as to centrosomes (Jeffers et al., 2007; Zhong et al., 2006); we observe no centrosomal localization for MCPH1 in syncytial embryos of *Drosophila*.

Mitotic arrest in *mcph1* syncytial embryos is a consequence of Chk2 activation

The defective mitotic spindles of embryos derived from *mcph1* females (hereafter referred to as '*mcph1* embryos') exhibit key features reminiscent of Chk2-mediated centrosomal inactivation. In particular, these spindles are short, barrel-shaped, anastral, and associated with poorly aligned chromosomes (Fig. 1). Late syncytial embryos of *Drosophila* use a two-stage response to DNA damage or replication defects (Sibon et al., 2000). The DNA checkpoint mediated by Meiotic 41 (MEI-41) and Grapes (GRP), the *Drosophila* orthologs of ATR (ATM-Rad3-related) and Chk1 kinases, respectively, delays mitotic entry via inhibitory phosphorylation of Cdk1 to

allow repair of DNA damage or completion of replication (Sibon et al., 1999; Sibon et al., 1997). When this checkpoint fails, a secondary damage-control system operating in mitosis is activated; resulting changes in spindle structure block chromosome segregation, presumably to stop propagation of defective DNA (Sibon et al., 2000; Takada et al., 2003). This damage-control system, known as centrosomal inactivation, is mediated by the checkpoint kinase Chk2 (Takada et al., 2003).

Loss of γ-tubulin from centrosomes of mitotic spindles is another characteristic feature of Chk2-mediated centrosomal inactivation. We detected decreased γ-tubulin staining of centrosomes during mitosis in *mcph1* embryos compared to wild type (supplementary material Fig. S3). We typically observe complete detachment of centrosomes from spindles in *mcph1* embryos. High levels of DNA damage induced by intense laser illumination can similarly cause complete centrosomal detachment from spindle poles of wild-type embryos (Takada et al., 2003), suggesting that the spindle changes we observe in *mcph1* embryos represent an extreme form of centrosomal inactivation.

To determine whether mitotic defects in *mcph1* embryos are due to Chk2-mediated centrosomal inactivation, we created lines doubly mutant for *mcph1* and *maternal nuclear kinase* (*mnk*), also known as *loki*, which encodes *Drosophila* Chk2 (Abdu et al., 2002; Brodsky et al., 2004; Masrouha et al., 2003; Xu et al., 2001). A similar approach has been used to demonstrate Chk2-mediated centrosomal inactivation in *grp*, *mei-41* and *wee1* embryos (Stumpff et al., 2004; Takada et al., 2003). Null *mnk* mutants are viable and fertile, but they are highly sensitive to ionizing radiation (Xu et al., 2001). Remarkably, we found that *mnk* suppresses many of the mitotic defects of *mcph1* embryos (Fig. 3A-D; Table 1). Mitotic spindles are restored to near-normality: in contrast to the short, barrel-shaped, anastral spindles of *mcph1* embryos, *mnk mcph1* embryos have elongated spindles with attached centrosomes. Thus, Chk2 activation contributes significantly to the *mcph1* phenotype in syncytial embryos.

In addition to suppressing the mitotic spindle defects of *mcph1* embryos, *mnk* strikingly suppresses their developmental arrest (Fig. 3G-K). Whereas *mcph1* embryos uniformly (100%) arrest in early to mid-syncytial cycles (cycles 1-8), most (>95%) *mnk mcph1* embryos complete syncytial divisions, cellularize, and cease developing near gastrulation. Thus, Chk2 activation causes *mcph1* embryos to arrest at the syncytial stage. Cellularized *mnk mcph1* embryos show irregularities in cell size and shape and intensity of DNA staining; gastrulation is grossly aberrant. We conclude that mutation of *mnk* removes the 'brakes' from *mcph1* embryos, allowing further nuclear divisions and development in the face of DNA defects, which eventually become so severe that embryos die peri-gastrulation.

mcph1 syncytial embryos exhibit a high frequency of chromatin bridging

We sought to understand the primary defects leading to Chk2 activation in *mcph1* embryos. Known triggers of Chk2-mediated centrosomal inactivation are mitotic entry with incompletely replicated or damaged DNA (Sibon et al., 2000; Takada et al., 2003). Although *mnk* suppresses many of the cell-cycle defects of *mcph1* embryos, we occasionally observe abnormal DNA aggregates shared by more than one spindle and multipolar spindles in *mnk mcph1* embryos that progress beyond the usual *mcph1* arrest point (Fig. 3E; Table 1). These defects are not observed in *mnk* embryos, suggesting that they are due to a lack of *mcph1*. In whole mounts of both *mnk mcph1* and *mcph1* embryos, we frequently observe chromatin bridging, which represents a physical linkage of chromosomes that prevents their segregation to opposite poles at anaphase (Fig. 3F; data not shown); this bridging could result from mitotic entry with unreplicated, damaged, and/or improperly condensed chromosomes. We were prohibited from quantifying this phenotype, however, as yolk proteins obscure nuclei that lie deep within the interior of early syncytial embryos. We circumvented this problem by adapting a larval

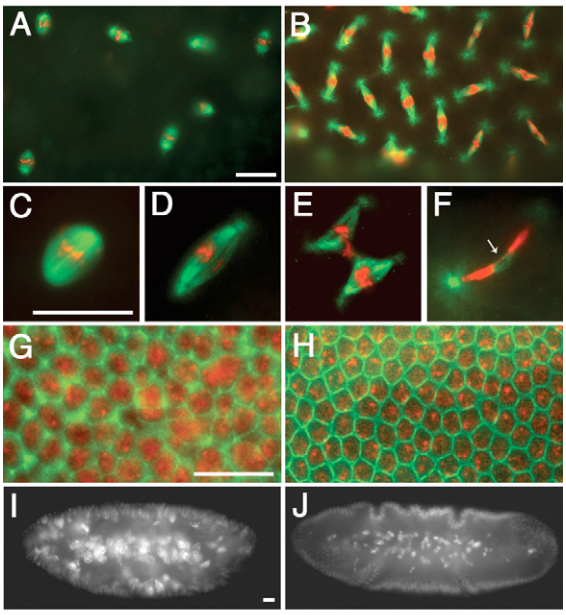

K

Genotype	Gastrulation[a] (% Embryos)	Embryos (n)
wild type	98.6	220
mcph1	0	200
mnk	83.3	180
mnk mcph1	95.9	170

[a]Embryos that initiate gastrulation

Fig. 3. Suppression of *mcph1* by *Chk2* (*mnk*). (A-J) Representative mitotic spindles in syncytial embryos and whole-mount embryos from $mcph1^{Z1861}$, *mnk* $mcph1^{Z1861}$ and wild-type females. Bars, 20 μm. (A-F) Microtubules are in green and DNA in red; low (A,B) and high (C-F) magnification views. *mcph1* embryos have *awol*-type (barrel-shaped, acentrosomal) spindles (A,C). *awol* phenotype is suppressed in *mnk mcph1* embryos (B,D): note restoration of elongated spindles and attached centrosomes. Other defects are seen in *mnk mcph1* embryos, such as DNA shared by two spindles (E) and DNA bridging (F, arrow). (G,H) Cellularized embryos (2-3 hours) stained for actin (green) and DNA (red). *mnk mcph1* embryos reach gastrulation with irregular cell size and DNA content (G) compared to wild type (H). (I,J) DNA-stained embryos (3-4 hours). *mnk mcph1* embryos (I) arrest peri-gastrulation with aberrant morphology compared to wild type (J). (K) Quantification of suppression of developmental arrest of $mcph1^{Z1861}$ embryos by *mnk*.

A

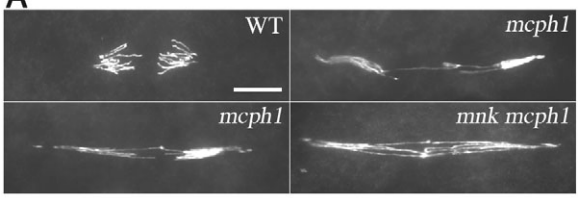

B

Genotype	Chromatin bridging (% A/T[a] figures)	Embryos (n[b])	Late A/T figures (n[b])
wild type	2.9	12	549
mcph1	68.3	14	60
mnk	10.6	6	113
mnk mcph1^{Z1861}	80.8	10	468

[a]A/T represents late anaphase to telophase.
[b]n represents the number of embryos or A/T figures scored.

Fig. 4. Chromatin bridging in *mcph1* embryos. Syncytial embryos were squashed and the DNA stained. (A) Representative late anaphase-to-telophase figures (images shown at same magnification). DNA bridging and increased pole-to-pole distances are seen in squashes of *mcph1*^{Z1861}/*mcph1*^{Z0978} and *mnk mcph1*^{Z1861} embryos. Bars, 10 μm. (B) Quantification of DNA bridging in *mcph1*^{Z1861}/*mcph1*^{Z0978} and *mnk mcph1*^{Z1861} embryo squashes. Wild-type and *mnk* embryos served as controls.

brain squash protocol for this developmental stage that allowed us to more clearly observe chromosomes of early embryos.

Using this approach, we found a high frequency of chromatin bridging in *mcph1* embryos (68% of late anaphase-to-telophase figures) in cycles 4-6, prior to their Chk2-mediated arrest (Fig. 4). Multiple bridges are often present between segregating chromosomes. Spindle pole-to-pole distances are increased dramatically compared to wild-type figures, presumably due to an extended anaphase B in a failed attempt to separate chromosomes that remain physically linked. All *mcph1* alleles reported here exhibit a similar degree of bridging, whereas this phenotype was rarely observed (<3%) in squashes of wild-type embryos (Fig. 4 and data not shown). Chromatin bridging probably represents a primary defect of *mcph1* embryos because it occurs at a similar frequency (81%) in *mnk mcph1* embryos that lack the Chk2-mediated checkpoint. We hypothesize that *mcph1* embryos incur chromosomal lesions that cause Chk2-mediated centrosomal inactivation and mitotic arrest as secondary consequences.

We occasionally observe apparent DNA breakage (evidenced by gaps in DAPI staining) along the length of bridging chromatin that is extensively stretched between poles in *mcph1* and *mnk mcph1* embryos (data not shown). We propose that DNA breakage is not a primary defect in *mcph1* embryos but rather occurs secondary to bridging. Our attempts to confirm the presence of DNA breaks in syncytial embryos (*mcph1* or irradiated wild type) by phospho-histone H2Av or TUNEL staining have been unsuccessful.

mcph1 is not required for the DNA checkpoint in *Drosophila*

Chk2-mediated centrosomal inactivation can be triggered in *Drosophila* syncytial embryos by DNA damaging agents, the DNA-replication inhibitor aphidicolin, or mutation of DNA checkpoint components (MEI-41 or GRP) or WEE1, a kinase that prohibits mitotic entry via inhibitory phosphorylation of Cdk1 (Sibon et al., 2000; Stumpff et al., 2004; Takada et al., 2003). Human *MCPH1*-deficient cells show defective G2-M and intra-S phase checkpoint responses following DNA damage (Alderton et al., 2006; Lin et al., 2005; Xu et al., 2004). In light of these studies linking human *MCPH1* to the ATR/Chk1 pathway and our results that *Drosophila mcph1* embryos undergo Chk2-mediated arrest, we sought to determine if MCPH1 is required for the DNA checkpoint in *Drosophila*.

Because MEI-41 and GRP are required during larval stages for the DNA checkpoint (Brodsky et al., 2000; Jaklevic and Su, 2004), we tested whether MCPH1 is required. In response to ionizing radiation (IR), eye-antennal imaginal disc cells of wild-type larvae undergo G2 arrest. We found that *mcph1* larvae also exhibit IR-induced G2 arrest under conditions in which *mei-41* larvae fail to arrest (Fig. 5A). We next tested the intra-S phase response to IR in larval brain cells. *mcph1* brains exhibited IR-induced intra-S phase arrest similar to that of wild type, whereas no arrest was seen in *mei-41* brains (Fig. 5B). We also tested sensitivity of *mcph1* larvae to hydroxyurea (HU), which blocks DNA replication. Under conditions in which no *mei-41* larvae survived, *mcph1* larvae were HU resistant, surviving at near-Mendelian ratios (Fig. 5C). We conclude that MCPH1 is not required for the DNA checkpoint in larval tissues. We also found that *mcph1* larvae, in contrast to *mei-41*, survive normally following low-dose IR exposure (Fig. 5D), indicating that MCPH1 is not required for DNA repair (Jaklevic and Su, 2004).

The MEI-41/GRP-mediated DNA-replication checkpoint is also developmentally activated at the midblastula transition (MBT) (Sibon et al., 1999; Sibon et al., 1997). Rapid S-M cycles of the early embryo are under maternal genetic control, and the switch to zygotic control occurs at the MBT after cycle 13. During late syncytial cycles (11-13), titration of a maternal DNA-replication factor is thought to induce a *mei-41*/*grp*-dependent checkpoint that causes Cdk1 inhibitory phosphorylation. Mitotic entry is thereby slowed, presumably to allow time to complete replication. Embryos from *mei-41* or *grp* females fail to lengthen interphase in late syncytial cycles and undergo extra S-M cycles (Sibon et al., 1999; Sibon et al., 1997).

We asked if MCPH1 is required for the MEI-41/GRP-dependent DNA-replication checkpoint at the MBT. *mcph1* embryos undergo arrest due to Chk2 activation prior to their reaching cortical divisions (cycles 10-13). Thus, to test whether *mcph1* is required for cell-cycle delay at the MBT, we performed live analysis of cortical divisions in *mnk mcph1* embryos that lack a functional Chk2-mediated checkpoint. We reasoned that any primary defects in cell-cycle timing due to mutation of *mcph1* would still be apparent in *mnk mcph1* embryos. This assumption is strengthened by a recent study showing that *mnk grp* embryos that progress through the MBT due to lack of Chk2-mediated arrest retain the cell-cycle timing defects of *grp* embryos (Takada et al., 2007). We monitored timing of nuclear envelope breakdown and reformation by differential interference contrast microscopy (DIC) and found no significant differences in interphase or mitosis lengths in *mnk mcph1* and wild-type embryos (Fig. 6A).

To further confirm that the DNA-replication checkpoint is

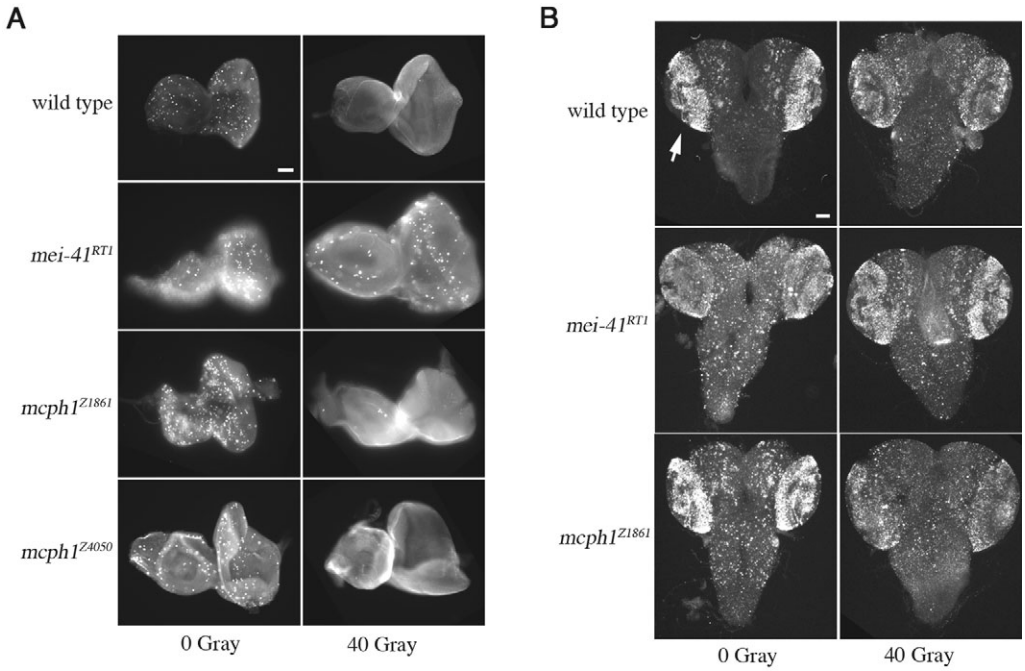

C

Sensitivity to hydroxyurea

Genotype	Percent homozygotes -HU	+HU
mei-41^{RT1}	59.2 (130)	0 (100)
mcph1^{Z1861}/ *mcph1*^{Z0978}	18.4 (163)	22.6 (288)
mcph1^{Exc21}	26.7 (101)	40.6 (101)

D

Eclosion after irradiation

Genotype	Percent eclosion 0 Gray	10 Gray
wild type	86.6 (134)	90.2 (153)
mei-41^{RT1}	79.8 (109)	3.3 (121)
mcph1^{Z1861}	85.1 (114)	82.4 (125)

Fig. 5. *mcph1* larvae have intact DNA checkpoints and normal sensitivity to DNA-damaging agents. (A,B) Cell-cycle checkpoints in *mcph1* larvae. Bars, 50 μm. (A) G2-M checkpoint. Eye-antennal imaginal disks were dissected from untreated (left) or irradiated (right) larvae, fixed, and stained with antibodies against phosphorylated Histone H3 (anti-PH3), a marker of mitotic cells. Lack of anti-PH3 staining post-IR indicates G2 arrest. Representative disks are shown (with at least twelve discs scored per genotype). (B) Intra-S phase checkpoint. Brains were dissected from untreated (left) or irradiated (right) larvae and labeled with BrdU. Decreased BrdU staining in brain lobes (arrows) post-IR indicates intra-S phase arrest. Representative brains are shown (with at least six brains scored per genotype). (C,D) Survival of *mcph1* larvae following exposure to DNA-damaging agents. (C) Sensitivity to hydroxyurea (HU). Larvae were grown on food minus or plus HU and allowed to develop. For each genotype, the ratio of homozygous mutant to total progeny is expressed as a percentage with total number of adult flies scored shown in parentheses. (D) Sensitivity to IR. Third instar larvae were untreated or exposed to low-dose irradiation and allowed to develop. For each genotype, the ratio of eclosed adults to total pupae is expressed as a percentage with total pupae shown in parentheses.

intact in *mnk mcph1* embryos, we assessed the extent of inhibitory phosphorylation of Cdk1 and found it to be comparable to that of wild type (Fig. 6B). We also found wild-type levels of Cyclin B and Cyclin A in *mnk mcph1* embryos (Fig. 6C; data not shown). Low levels of Chk1 protein have been reported in *MCPH1* siRNA human cells (Lin et al., 2005; Xu et al., 2004), but we detected normal levels of Grapes (Chk1) in *mcph1* and *mnk mcph1* embryos (Fig. 6D). Thus, our data do not support a role for *Drosophila* MCPH1 in control of cell-cycle timing in syncytial embryos via regulation of Cdk1 phosphorylation, Cyclin B, or Grapes levels.

mcph1 cooperates with *mei-41* and *grp* to regulate syncytial divisions

Previous studies of *grp* and *mei-41* embryos largely focused on mitotic defects in cortical nuclear divisions, which are amenable to live analysis (Sibon et al., 2000; Takada et al., 2003). Given the earlier arrest point of *mcph1* embryos, we initially concluded that *mcph1* and *mei-41*/*grp* must have discrete roles. We subsequently found, however, that a sizeable fraction of embryos (17-33%) from homozygous or hemizygous *grp* females arrest in pre-cortical cycles (1-9) with acentrosomal, barrel-shaped spindles nearly identical to that of *mcph1* (Fig. 7A). We obtained similar results for all three *grp* alleles tested (Fig. 7B), including the null *grp*^{209} (Larocque et al., 2007). Our data and a previous report of defective Cyclin A proteolysis in pre-cortical *grp* embryos (Su et al., 1999) have established a role for *grp* in regulating the cell cycles of early syncytial embryos. We also found that *mcph1* dominantly enhances a weak *mei-41* phenotype to a degree similar to that of *grp* (Fig. 7C). Intriguingly, by immunoblotting, we consistently observe an upward mobility shift in MCPH1 in *grp* or *mei-41* embryonic extracts (Fig. 7D). Taken together, these data suggest that MCPH1 cooperates with MEI-41 and GRP to regulate the cell cycles of the early embryo via a mechanism independent of Cdk1 phosphorylation.

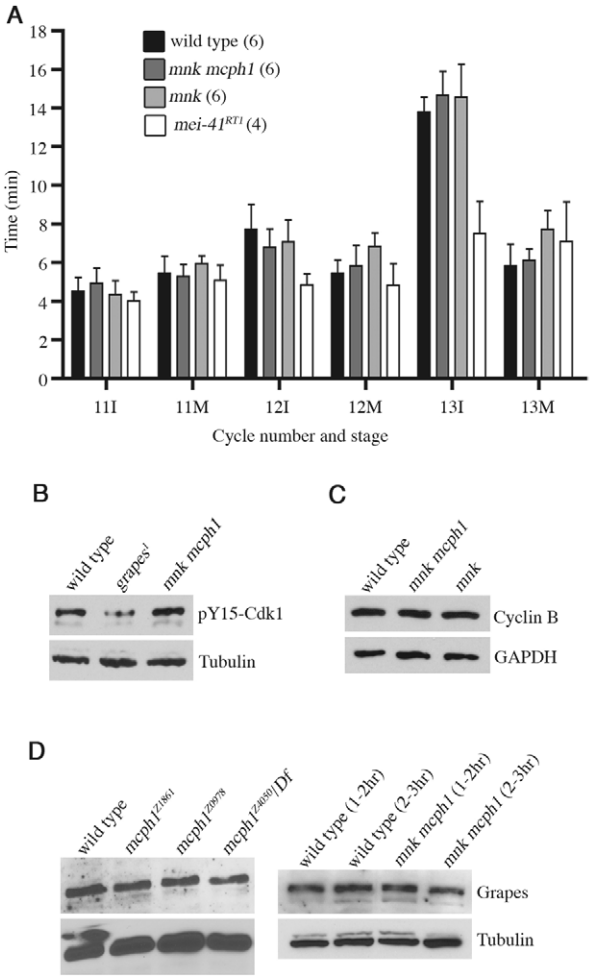

Fig. 6. Intact DNA-replication checkpoint and normal Cyclin B levels in *mcph1* embryos. (A) Quantification of cell-cycle timing during cortical divisions of early embryogenesis. No significant differences in interphase (I) or mitosis (M) lengths were observed for *mnk mcph1*^{Z1861} embryos compared to wild-type or *mnk* controls, whereas shorter interphases were apparent in *mei-41* embryos (cycles 12 and 13). Average times with standard deviations (error bars) are shown. Numbers of embryos scored for each genotype are shown in parentheses. (B) Western analysis using phospho-specific antibodies against Cdk1 reveals wild-type levels of pY15-Cdk1 in extracts of *mnk mcph1*^{Z1861} embryos (1-2 hours). Control *grp* embryos have reduced pY15-Cdk1 levels. (C) Western analysis reveals normal Cyclin B levels in *mnk mcph1*^{Z1861} embryos (1-2 hours). (D) Western analysis reveals normal GRP levels in *mcph1* and *mnk mcph1*^{Z1861} embryos (1-2 hours unless otherwise indicated). Loading controls: anti-α-tubulin or anti-GAPDH.

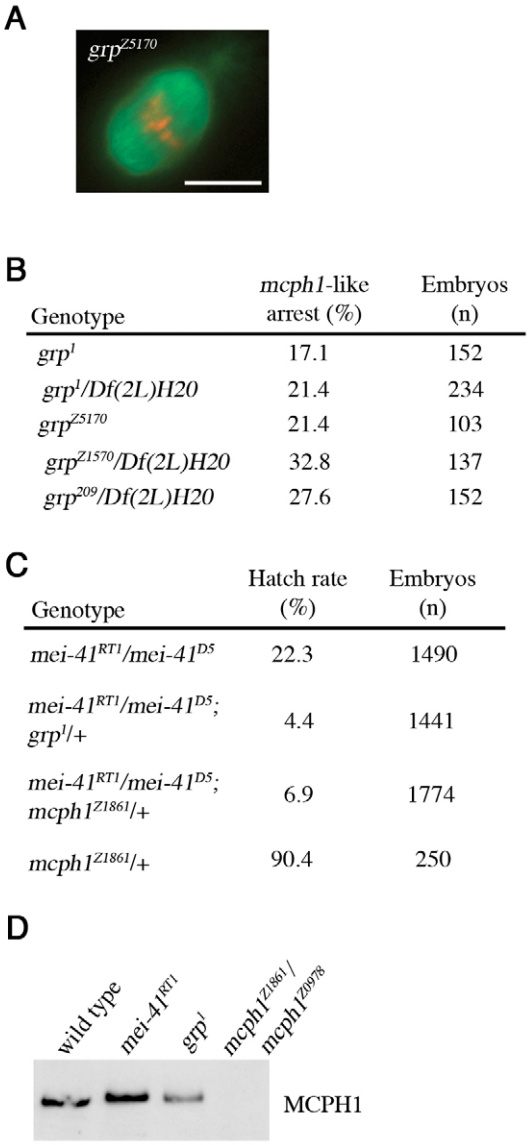

B

Genotype	*mcph1*-like arrest (%)	Embryos (n)
grp^{1}	17.1	152
grp^{1}*/Df(2L)H20*	21.4	234
grp^{Z5170}	21.4	103
grp^{Z1570}*/Df(2L)H20*	32.8	137
grp^{209}*/Df(2L)H20*	27.6	152

C

Genotype	Hatch rate (%)	Embryos (n)
mei-41^{RT1}*/mei-41*^{D5}	22.3	1490
mei-41^{RT1}*/mei-41*^{D5}*; grp*^{1}*/+*	4.4	1441
mei-41^{RT1}*/mei-41*^{D5}*; mcph1*^{Z1861}*/+*	6.9	1774
mcph1^{Z1861}*/+*	90.4	250

Fig. 7. *mcph1* cooperates with *mei-41* and *grp* in the early embryo. (A) Mitotic spindle from a pre-cortically arrested *grapes*^{Z5170} embryo resembles *awol*-type spindles of *mcph1* embryos. Microtubules are in green and DNA in red. Scale bar: 10 μm. (B) Quantification of *mcph1*-like arrest in *grp* embryos (2-4 hours). (C) *mcph1* dominantly enhances *mei-41* embryonic lethality. Introduction of one copy of *mcph1*^{Z1861} into a semi-sterile *mei-41* background (*mei-41*^{RT1}*/mei-41*^{D5}) reduces embryonic hatch rate more than threefold. (D) Immunoblotting shows slower gel mobility of MCPH1 in *mei-41*^{RT1} or *grp*^{1} embryos (1-2 hours) relative to wild type.

mcph1 males exhibit defects in adult brain structure

On the basis of the reduced brain size of patients with mutation of *mcph1*, we tested whether mutation of *Drosophila mcph1* affects brain development. We did not observe an obvious change in overall brain size, but we did observe morphological defects in central brain structures. The mushroom bodies (MBs) of the *Drosophila* adult brain are bilaterally symmetrical structures required for olfactory memory and other complex adaptive behaviors (de Belle and Heisenberg, 1994). MB structure is stereotyped, and gross morphological brain defects often uncover structural defects in MBs. The 2500 intrinsic neurons in each MB can be subdivided into at least three morphologically well-defined subsets (αβ, α′β′ or γ) based on bundling of their axonal projections in the region of the MBs called the lobes (Crittenden et al., 1998). Each MB neuron contributing to the αβ subdivision bifurcates and sends one axon branch vertically to the α lobe and one horizontally to the β lobe. Anti-Fasciclin II (FasII) antibodies strongly

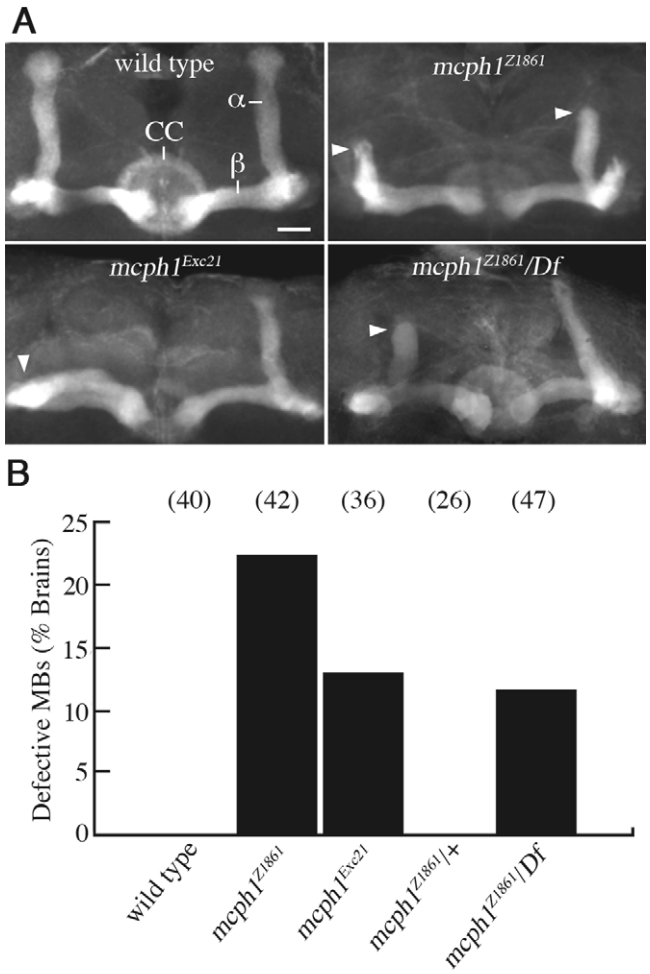

Fig. 8. Defects in male *mcph1* brains. Adult male brains were stained with anti-FasII antibodies to visualize mushroom body (MB) αβ lobes and the ellipsoid body of the central complex (CC). (A) MB αβ lobes of wild-type brains are symmetric, whereas MBs of *mcph1* brains are occasionally defective with missing or diminished αβ lobes (arrowheads). *Df=Df(2R)BSC39*, which removes the *mcph1* genomic locus. (B) Quantification of brain defects in *mcph1* males. Sample number for each genotype is indicated in parentheses (top).

label MB neurons that lie in the αβ lobes (Grenningloh et al., 1991), thereby allowing straightforward visualization of developmental defects.

Our initial analysis revealed obvious morphological MB defects in brains of $mcph1^{Z1861}$ and $mcph1^{Exc21}$ male flies (Fig. 8A). The nature of the MB defects was variable, ranging from missing or malformed lobes to complete absence of lobes, and defects were often asymmetric. For unknown reasons, we never observed MB defects in brains of female *mcph1* flies (data not shown). Quantification revealed defects in 22% of $mcph1^{Z1861}$ and 13% of $mcph1^{Exc21}$ male brains (Fig. 8B). We similarly found defects in 11.5% of brains from males carrying $mcph1^{Z1861}$ in trans to a deletion of the *mcph1* genomic locus; no defects were found in control heterozygous ($mcph1^{Z1861}$/+) male brains. These data establish a role for *mcph1* in *Drosophila* brain development.

Discussion

We identified *Drosophila mcph1*, the homolog of the human primary microcephaly gene *MCPH1*, in a genetic screen for cell-cycle regulators and have shown that it is required for genomic stability in the early embryo. Three additional primary microcephaly (*MCPH*) genes have been identified in humans: *ASPM*, *CDK5RAP2*, and *CENPJ* (reviewed by Cox et al., 2006). Much of our understanding of the biological functions of the proteins encoded by human *MCPH* genes has come from studies of their *Drosophila* counterparts. Mutation of *abnormal spindle* (*asp*), the *Drosophila* ortholog of *ASPM*, results in cytokinesis defects and spindles with poorly focused poles (do Carmo Avides and Glover, 1999; Wakefield et al., 2001). The *Drosophila* ortholog of *CDK5RAP2*, *centrosomin* (*cnn*), is required for proper localization of other centrosomal components (Li and Kaufman, 1996; Megraw et al., 1999). *Sas-4*, the *Drosophila* ortholog of *CENPJ*, is essential for centriole production, and the mitotic spindle is often misaligned in asymmetrically dividing neuroblasts of *Sas-4* larvae (Basto et al., 2006). Whereas all of these primary microcephaly genes are critical regulators of spindle and centrosome functions, mitotic defects in *Drosophila mcph1* mutants are largely secondary to Chk2 activation in response to DNA defects; thus, *mcph1* probably represents a distinct class of primary microcephaly genes.

MCPH1 is a BRCT domain-containing protein, suggesting that it plays a role in the DNA damage response. Conflicting models of MCPH1 function, however, have emerged from studies of human cells as it has been proposed to function at various levels in this pathway: upstream, at the level of damage-induced foci formation (Rai et al., 2006) and further downstream, to augment phosphorylation of targets by the effector Chk1 (Alderton et al., 2006). The phenotype of embryos from null *mcph1* females is more severe than that of embryos from null *grp* females, suggesting that enhancement of phosphorylation of GRP (Chk1) substrates is not the sole function of MCPH1. Furthermore, we found both the DNA checkpoint in larval stages and its developmentally regulated use at the MBT to be intact in *mcph1* mutants, suggesting a requisite role for MCPH1 in the DNA checkpoint evolved in higher organisms.

Studies of human cells suggest a role for MCPH1 in regulation of chromosome condensation. Microcephalic patients homozygous for a severely truncating mutation in MCPH1 show increased frequency of G2-like cells displaying premature chromosome condensation (PCC) with an intact nuclear envelope (Alderton et al., 2006; Trimborn et al., 2004). Depletion of Condensin II subunits by RNAi in *MCPH1*-deficient cells leads to reduction in the frequency of PCC, suggesting that MCPH1 is a negative regulator of chromosome condensation (Trimborn et al., 2006). Alderton et al. (Alderton et al., 2006) observed a decreased level of inhibitory phosphates on Cdk1 that correlated with PCC in *MCPH1*-deficient cells. The authors proposed that MCPH1 maintains Cdk1 phosphorylation in an ATR-independent manner because PCC is not seen in cells of patients with Seckel syndrome, which is caused by mutation of *ATR*; residual ATR present in these cells, however, may be sufficient to prevent PCC (O'Driscoll et al., 2003). Furthermore, in several experimental systems, ATR and Chk1 have been implicated in an S-M checkpoint that prevents premature mitotic entry with

unreplicated DNA (reviewed by Petermann and Caldecott, 2006).

We have shown that embryos from *grp* (*Chk1*) females occasionally undergo *mcph1*-like arrest in early syncytial cycles, prior to the time at which inhibitory phosphorylation of Cdk1 is thought to control mitotic entry. Thus, decreased signaling through the DNA checkpoint resulting in less Cdk1 phosphorylation is unlikely to explain this *mcph1*-like arrest. In contrast to studies of *MCPH1*-deficient human cells, we detect no decrease in pY15-Cdk1 levels in *mcph1* embryos allowed to progress beyond their normal arrest point by mutation of *mnk* (*Chk2*). Based on these data and the PCC phenotype associated with loss of *MCPH1* in humans, we propose a model in which MEI-41/GRP cooperate with MCPH1 in syncytial embryos in a Cdk1-independent manner to delay chromosome condensation until DNA replication is complete (Fig. 9). In the absence of *mcph1*, we hypothesize that embryos condense chromosomes before finishing S phase, resulting in DNA defects (bridging chromatin), Chk2 activation, and mitotic arrest. We were precluded from directly monitoring chromosome condensation in *mnk mcph1* embryos expressing Histone-GFP as previously described (e.g. Brodsky et al., 2000) because we were unable to establish fly stocks carrying this transgene in the *mnk* background. Live imaging of *mcph1* embryos was not technically feasible because they arrest prior to cortical stages, and yolk proteins obscure more interior nuclei in early embryos. *grp* embryos have been reported to initiate chromosome condensation with normal kinetics (Yu et al., 2000), although a subtle PCC phenotype might be difficult to detect.

Support for our model that MCPH1 allows completion of S phase by delaying chromosome condensation comes from the observation that inhibition of DNA replication in syncytial embryos (via injection of aphidicolin or HU) results in phenotypes similar to those observed in *mcph1* embryos, including chromatin bridging, which is presumably a direct consequence of progressing through mitosis with unreplicated chromosomes (Raff and Glover, 1988), and Chk2 activation (Takada et al., 2003). Alternatively, *mcph1* might be required during S phase for timely completion of DNA synthesis; in this case, *mcph1* embryos would initiate chromosome condensation with normal kinetics prior to completing replication. Coordination of S-phase completion and mitotic entry may be particularly critical in the rapid cell cycles of the early embryo that lack gap phases and may explain why loss of *Drosophila mcph1* is most apparent at this developmental stage. Interestingly, even in the absence of exogenous genotoxic stress, *MCPH1*-deficient human cells also exhibit a high frequency of chromosomal aberrations (Rai et al., 2006), which may be a consequence of PCC.

An evolutionary role for *mcph1* in expansion of brain size along primate lineages has emerged in recent years (reviewed by Woods et al., 2005). In brains of *Drosophila mcph1* males, we find low-penetrance defects in MB structure. Both MCPH1 isoforms are expressed in larval brains, and all *mcph1* mutations described here affect both isoforms, so it is unclear whether MB formation requires one or both isoforms. The lack of MB defects in *mcph1* females is puzzling because both isoforms are found in male and female larval brains (data not shown); other sex-specific factors are probably involved. Larval brains of *mcph1* males show no obvious aneuploidy (data not shown) or spindle orientation defects (Andrew Jackson, personal communication), so the cellular basis for these defects remains to be determined. It will be interesting to test in future studies whether *mei-41* and *grp*, which cooperate with *mcph1* to regulate early embryogenesis, are similarly required in *Drosophila* males for brain development.

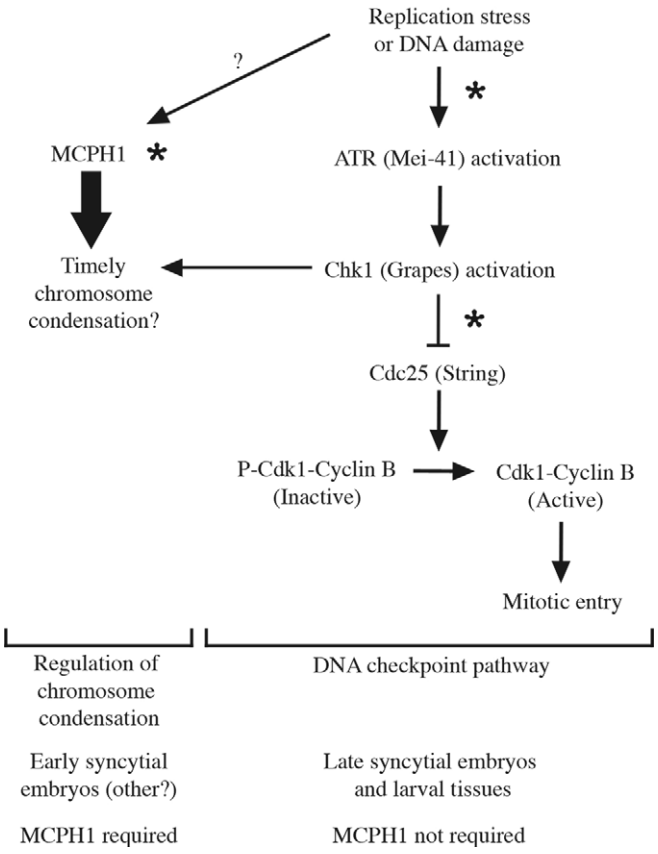

Fig. 9. Proposed model of *Drosophila* MCPH1 function. Asterisks represent key points at which human MCPH1 reportedly functions. Our data suggest that MCPH1 cooperates with MEI-41/GRP in a Cdk1-independent manner to promote genomic integrity in embryos, possibly by controlling timing of chromosome condensation.

In conclusion, we have demonstrated an essential role for *Drosophila* MCPH1 in maintaining genomic integrity in the early embryo. Our data suggest that, in contrast to the mammalian protein, *Drosophila* MCPH1 is not required for the DNA checkpoint, although its role in regulating other processes (e.g. chromosome condensation) may be conserved. We predict that the early embryo of *Drosophila* will continue to be an important model genetic system for unraveling the biological functions of MCPH1, a critical determinant of brain size in humans.

Materials and Methods

Drosophila stocks

Flies were maintained at 25°C using standard techniques (Greenspan, 2004). Wild-type stocks used were *y w* or *Oregon-R*. Zuker alleles of *mcph1* are *cn bw* and balanced over *CyO*. Zuker stock designations have been shortened and superscripted to indicate that they are alleles of *mcph1* (e.g. *ZII-1861* becomes $mcph1^{ZI861}$). Deficiency strains, P-element lines for mapping, mutants for complementation

testing (*grp*^{1}, *aurora*^{1}, *wee1*^{ES1}), *nanos-Gal4:VP16* stock, and *mei-41* mutants were from Bloomington Stock Center. *mcph1* P-element insertions were from Bloomington Stock Center (*EY11307*), Kyoto Stock Center (*NP6229-5-1*), or a gift from Steven Hou (*l(2)SH0220*). *tefu*^{356}, *mnk*^{6006} and *grp*^{209} stocks were gifts from Mike Brodsky, Bill Theurkauf and Tin Tin Su, respectively.

Identification of new alleles of cell-cycle regulators

A combination of female meiotic recombination, deficiency mapping and direct complementation testing of candidates was used to identify mutants from our screen. Complementation testing with known cell-cycle regulators was performed by assessing fertility of females carrying a Zuker chromosome in trans to a known mutation. We used the following alleles: *wee1*^{ES1} (Price et al., 2000), *grp*^{1} (Fogarty et al., 1997), *tefu*$^{\Delta 356}$ (Oikemus et al., 2004) and *aur*^{1} (Glover et al., 1995).

Quantification of embryonic hatch rates

For hatch rate assays, embryos (0-4 hours) were collected on grape plates, counted and aged ~40 hours at 25°C. The number of hatched embryos was determined by subtracting the number of unhatched (intact) embryos from the total number collected. Hatch rate is the ratio of hatched to total embryos expressed as a percentage.

Genetic and molecular mapping of *awol*

The *awol* gene was localized by a combination of mapping strategies. We first screened a collection of deficiencies on the second chromosome for non-complementation of the female sterility of *awol*^{Z1861}. We found that females carrying *awol*^{Z1861} in trans to *Df(2R)BSC39* produced embryos with the awol phenotype; similar results were obtained for *awol*^{Z0978} and *awol*^{iZ4050}. Thus, *awol* lies between the breakpoints of *Df(2R)BSC39* in the polytene interval 48C5-E1, a region that contains ~35 genes. We mapped *awol* by P-element-induced male recombination (Chen et al., 1998) relative to the following insertion lines: *Mtor*^{k03905}, *ERp60*^{BG01854}, *KG04952*, *otk*^{EP2017} and *CG8378*^{EP2501}. We thereby narrowed *awol* to a region of five genes (including *mcph1*) that lie distal to *ERp60*^{BG01854} and proximal to *KG04952*. The *awol* stock used (*cn ZII-1861 bw/CyO*) has visible flanking markers *cn* and *bw*. The source of transposase was *Delta2-3 Sb*. Multiple independent recombinant chromosomes were recovered for each P-element line tested. Genomic DNA was extracted from whole flies homozygous for *awol* mutations essentially as previously described (Ballinger and Benzer, 1989). *mcph1* coding regions were PCR-amplified from genomic DNA and sequenced.

Generation of *mcph1* excision line

P-element insertions have been identified in the 5′-UTR of *mcph1* (*NP6229-5-1*) and within its largest intron (*l(2)k06612*, *l(2)SH0220* and *EY11307*) (Grumbling and Strelets, 2006). *l(2)k06612* is no longer available from stock centers. We mapped the lethality of line *l(2)SH0220* (Oh et al., 2003) outside of the *mcph1* genomic region (data not shown). We found that *EY11307* homozygous and *EY11307/mcph1*^{Z1861} transheterozygous females are viable, fertile and produce embryos with nearly wild-type levels of MCPH1 protein, indicating that this P-insertion has little effect on *mcph1* transcription; similar results were obtained for *NP6229-5-1* (data not shown). *EY11307* is inserted in the 5′-UTR of *CG13189*, which encodes a putative metal ion transporter, and the largest intron of *mcph1* (Fig. 2A). All EMS-induced *mcph1* mutations described here lie outside of *CG13189* (including two beyond its 3′ end), thereby making it unlikely that decreased *CG13189* activity causes the awol phenotype. We performed imprecise P-element excision of *EY11307* to generate *mcph1*^{Exc21}, which lacks two internal exons and part of the 3′-most exon of *mcph1*; this excision left the 5′-UTR, coding region and 3′-UTR of *CG13189* intact, but probably removed some of its promoter (Fig. 2A).

Embryo fixation, staining and microscopy

Embryos (1-2 hours unless otherwise indicated) were collected for staining using standard techniques (Rothwell and Sullivan, 2000). For mouse anti-α-tubulin (DM1α, 1:500, Sigma) or rabbit anti-Centrosomin (1:10,000, a gift from W. Theurkauf) staining, embryos were dechorionated in 50% bleach, fixed, and devitellinized by shaking in a mixture of methanol and heptane (1:1). For staining with guinea pig anti-MCPH1 (1:200) or mouse anti-actin (1:400, MP Biomedicals) or co-staining with anti-α-tubulin (YL1/2, Serotec, 1:250) and anti-γ-tubulin (GTU-88, 1:250, Sigma), embryos were fixed fore 20 minutes in a mixture of 3.7% formaldehyde in PBS and heptane (1:1). The aqueous layer containing formaldehyde was removed and embryos devitellinized as described above. Embryos were incubated in primary antibodies at 4°C overnight except for anti-MCPH1 (4°C for three days). Secondary antibodies were conjugated to Cy2 (Jackson ImmunoResearch). Embryos were stained with propidium iodide (Sigma) and cleared as previously described (Fenger et al., 2000). A Nikon Eclipse 80i microscope equipped with a CoolSNAP ES camera (Photometrics) and Plan-Apo (20×, 100×) or Plan-Fluor 40× objectives was used; for confocal images, we used a Zeiss LSM510 microscope equipped with a Plan-Neofluar 100× objective.

Embryo squashes and quantification of DNA bridging

Methanol-fixed embryos (40-80 minutes) were placed in 2-μl drops of 45% acetic acid on coverslips for 1-2 minutes. Slides were lowered onto coverslips, inverted and embryos squashed by hand between blotting paper. Samples were snap-frozen in liquid nitrogen, coverslips removed, and slides immersed in ethanol at –20°C for 10 minutes and air-dried. Vectashield mounting medium with DAPI (Vector Labs) and new coverslips were added to slides. Fluorescence microscopy (100× objective) was used to visualize DNA. Late anaphase and telophase figures (cycle-5 to -7 embryos) were examined. The presence of one or more linkages between DNA masses segregating to opposite poles was scored as a bridging defect.

Live embryo imaging

For analysis of cell-cycle timing, embryos (0-1.5 hours) were dechorionated in 50% bleach, glued (octane extract of tape) to glass-bottomed culture dishes (MatTek Corp.), and covered with halocarbon oil 27 (Sigma). DIC images of dividing embryos at 21.5-22.5°C were captured (20-second intervals) using a Nikon Eclipse TE2000-E inverted microscope with a CoolSNAP HQ CCD camera (Photometrics), Plan-Apo 20× objective, and IPLab image acquisition software (BD Biosciences). Interphase length was determined by counting frame numbers from nuclear envelope formation to breakdown. Mitosis length was determined by counting frame numbers from nuclear envelope breakdown to reformation. Cycle number was determined by nuclear size and density.

mcph1 cDNA clones and transgenes

cDNA clones encoding MCPH1-B (LD43341) or MCPH1-A (LP15451) were from the Drosophila Gene Collection or Drosophila Genomics Resource Center, respectively. MCPH1-B coding region was PCR-amplified from LD43341, subcloned into UASp (Rorth, 1998), and transformed into *y w* flies (Spradling, 1986). To generate IVT constructs, MCPH1-B coding region was subcloned into pCS2. The BRCT domains of MCPH1 were identified using ScanProsite. Descriptions of FlyBase's annotation of *mcph1* were based on version FB2006_01 (Grumbling and Strelets, 2006). GenBank accession number for LP15451 encoding MCPH1-A is EF587234.

Polyclonal antibodies against MCPH1

Maltose-binding protein (MBP) fused to MCPH1-B protein (residues 1-352) was used to produce antibodies. N-terminal MCPH1-B sequence was PCR-amplified from LD43341 and subcloned into pMAL (New England Biolabs). MBP-N-MCPH1-B was made in bacterial cells, purified using amylose beads, and injected into guinea pigs for antibody production (Covance). Anti-MCPH1 antibodies were affinity purified using standard techniques.

Protein extracts and immunoblots

Protein extracts were made by homogenizing either embryos (1-2 hours old unless otherwise indicated) or dissected tissues in urea sample buffer as described previously (Tang et al., 1998). Proteins were transferred to nitrocellulose for immunoblotting using standard techniques. MCPH1-A and -B (unlabeled proteins) were made by coupled transcription-translation of LP15451 and LD43341, respectively, according to the manufacturer's protocol (Promega). Antibodies were used as follows: guinea pig anti-MCPH1 (1:200-500), mouse anti-Cyclin B (F2F4, 1:200, Developmental Studies Hybridoma Bank), rabbit anti-pY15-Cdk1 (1:1000, Upstate), rabbit anti-Grapes (1:500, a gift from T. T. Su) (Purdy et al., 2005), mouse anti-α-tubulin (DM1α, 1:5000, Sigma), mouse anti-GAPDH (1:1000, Abcam). HRP-conjugated secondary antibodies and chemiluminescence were used to detect primary antibodies.

DNA damage response assays

We used a Mark I cesium-137 irradiator as a source of irradiation (IR). To test the G2-M checkpoint post-IR, we used the method of Brodsky et al. (Brodsky et al., 2000) except that fluorescently coupled secondary antibodies were used. To test the intra-S phase checkpoint post-IR, we used the method of Jaklevic and Su (Jaklevic and Su, 2004) except that larvae were exposed to 40 Gray (4000 Rad). To test sensitivity to irradiation, third instar larvae were untreated or exposed to 10 Gray (1000 Rad), transferred to food, and allowed to pupate and eclose as adults. Mutant chromosomes were balanced over *CyO, arm-GFP* (Sullivan et al., 2000) and homozygotes identified by lack of GFP signal. Numbers of pupae formed and empty pupal cases (due to eclosion) were scored up to 10 days post-IR. Percentage eclosion (measure of survival) is the number of empty pupal cases expressed as a percentage of total pupae. All irradiated larvae formed pupae in these experiments. To test hydroxyurea (HU) sensitivity, heterozygous adults (ten males and ten virgin females) were added to vials. After embryo collection (48 hours), adults were removed and 500 ml of 20 μM HU in water was added to food 24 hours later. Adult progeny were scored after 2 weeks. HU sensitivity is indicated by preferential loss of a specific genotypic class.

Adult brain immunostaining

Adult brains were fixed, immunostained and examined by confocal microscopy as previously described (Krashes et al., 2007) using mouse anti-Fasciclin II antibodies (1D4, 1:4, Developmental Studies Hybridoma Bank).

The maternal-effect mutant collection was kindly provided by Charles Zuker. We thank Edmund Koundakjian, David Cowan and Robert Hardy for establishing the collection and the labs of Barbara Wakimoto, Dan Lindsley and Mike McKeown for identifying the female-sterile subset. We gratefully acknowledge Terry Orr-Weaver, in whose lab the screen was performed (with support from NIH grant GM39341 and NSF grant MCB0132237 to T.O.-W.) and her lab members for participation in the screen. We thank Irina Kaverina and Saeko Takada for expert advice on live analysis of embryos by DIC microscopy. Erin Loggins, Audrey Frist and Joshua Tarkoff provided technical assistance. Curtis Thorne helped map *awol*. Bill Theurkauf, Tin Tin Su and Mike Brodsky provided antibodies and fly stocks. We thank Bill Theurkauf and Tin Tin Su for helpful discussions and Andrew Jackson for sharing unpublished data. Daniela Drummond-Barbosa, Andrea Page-McCaw, Terry Orr-Weaver and members of the Lee lab provided critical comments on the manuscript. This work was supported by a Basil O'Connor Starter Scholar Research Award (Grant 5-FY05-29) and Grant 1-FY07-456 from the March of Dimes Foundation and NIH grant GM074044 to L.A.L.

References

Abdu, U., Brodsky, M. and Schupbach, T. (2002). Activation of a meiotic checkpoint during Drosophila oogenesis regulates the translation of Gurken through Chk2/Mnk. *Curr. Biol.* **12**, 1645-1651.

Alderton, G. K., Galbiati, L., Griffith, E., Surinya, K. H., Neitzel, H., Jackson, A. P., Jeggo, P. A. and O'Driscoll, M. (2006). Regulation of mitotic entry by microcephalin and its overlap with ATR signalling. *Nat. Cell Biol.* **8**, 725-733.

Ballinger, D. G. and Benzer, S. (1989). Targeted gene mutations in Drosophila. *Proc. Natl. Acad. Sci. USA* **86**, 9402-9406.

Bartek, J. (2006). Microcephalin guards against small brains, genetic instability, and cancer. *Cancer Cell* **10**, 91-93.

Basto, R., Lau, J., Vinogradova, T., Gardiol, A., Woods, C. G., Khodjakov, A. and Raff, J. W. (2006). Flies without centrioles. *Cell* **125**, 1375-1386.

Brand, A. H. and Perrimon, N. (1993). Targeted gene expression as a means of altering cell fates and generating dominant phenotypes. *Development* **118**, 401-415.

Brodsky, M. H., Sekelsky, J. J., Tsang, G., Hawley, R. S. and Rubin, G. M. (2000). mus304 encodes a novel DNA damage checkpoint protein required during Drosophila development. *Genes Dev.* **14**, 666-678.

Brodsky, M. H., Weinert, B. T., Tsang, G., Rong, Y. S., McGinnis, N. M., Golic, K. G., Rio, D. C. and Rubin, G. M. (2004). Drosophila melanogaster MNK/Chk2 and p53 regulate multiple DNA repair and apoptotic pathways following DNA damage. *Mol. Cell. Biol.* **24**, 1219-1231.

Chen, B., Chu, T., Harms, E., Gergen, J. P. and Strickland, S. (1998). Mapping of Drosophila mutations using site-specific male recombination. *Genetics* **149**, 157-163.

Cox, J., Jackson, A. P., Bond, J. and Woods, C. G. (2006). What primary microcephaly can tell us about brain growth. *Trends Mol. Med.* **12**, 358-366.

Crittenden, J. R., Skoulakis, E. M., Han, K. A., Kalderon, D. and Davis, R. L. (1998). Tripartite mushroom body architecture revealed by antigenic markers. *Learn. Mem.* **5**, 38-51.

de Belle, J. S. and Heisenberg, M. (1994). Associative odor learning in Drosophila abolished by chemical ablation of mushroom bodies. *Science* **263**, 692-695.

do Carmo Avides, M. and Glover, D. M. (1999). Abnormal spindle protein, Asp, and the integrity of mitotic centrosomal microtubule organizing centers. *Science* **283**, 1733-1735.

Fenger, D. D., Carminati, J. L., Burney-Sigman, D. L., Kashevsky, H., Dines, J. L., Elfring, L. K. and Orr-Weaver, T. L. (2000). PAN GU: a protein kinase that inhibits S phase and promotes mitosis in early Drosophila development. *Development* **127**, 4763-4774.

Foe, V. E., Odell, G. M. and Edgar, B. A. (1993). Mitosis and morphogenesis in the *Drosophila* embryo: point and counterpoint. In *The Development of Drosophila melanogaster* (ed. M. Bate and A. Martinez Arias), pp. 149-300. Cold Spring Harbor, NY: Cold Spring Harbor Laboratory Press.

Fogarty, P., Campbell, S. D., Abu-Shumays, R., Phalle, B. S., Yu, K. R., Uy, G. L., Goldberg, M. L. and Sullivan, W. (1997). The Drosophila grapes gene is related to checkpoint gene chk1/rad27 and is required for late syncytial division fidelity. *Curr. Biol.* **7**, 418-426.

Freeman, M., Nusslein-Volhard, C. and Glover, D. M. (1986). The dissociation of nuclear and centrosomal division in gnu, a mutation causing giant nuclei in Drosophila. *Cell* **46**, 457-468.

Glover, D. M., Leibowitz, M. H., McLean, D. A. and Parry, H. (1995). Mutations in aurora prevent centrosome separation leading to the formation of monopolar spindles. *Cell* **81**, 95-105.

Glover, J. N., Williams, R. S. and Lee, M. S. (2004). Interactions between BRCT repeats and phosphoproteins: tangled up in two. *Trends Biochem. Sci.* **29**, 579-585.

Greenspan, R. J. (2004). *Fly Pushing: The Theory and Practice of Drosophila Genetics*. Cold Spring Harbor, NY: Cold Spring Harbor Laboratory Press.

Grenningloh, G., Rehm, E. J. and Goodman, C. S. (1991). Genetic analysis of growth cone guidance in Drosophila: fasciclin II functions as a neuronal recognition molecule. *Cell* **67**, 45-57.

Grumbling, G. and Strelets, V. (2006). FlyBase: anatomical data, images and queries. *Nucleic Acids Res.* **34**, D484-D488.

Huyton, T., Bates, P. A., Zhang, X., Sternberg, M. J. and Freemont, P. S. (2000). The BRCA1 C-terminal domain: structure and function. *Mutat. Res.* **460**, 319-332.

Jackson, A. P., Eastwood, H., Bell, S. M., Adu, J., Toomes, C., Carr, I. M., Roberts, E., Hampshire, D. J., Crow, Y. J., Mighell, A. J. et al. (2002). Identification of microcephalin, a protein implicated in determining the size of the human brain. *Am. J. Hum. Genet.* **71**, 136-142.

Jaklevic, B. R. and Su, T. T. (2004). Relative contribution of DNA repair, cell cycle checkpoints, and cell death to survival after DNA damage in Drosophila larvae. *Curr. Biol.* **14**, 23-32.

Jeffers, L. J., Coull, B. J., Stack, S. J. and Morrison, C. G. (2007). Distinct BRCT domains in Mcph1/Brit1 mediate ionizing radiation-induced focus formation and centrosomal localization. *Oncogene* doi:10.1038/sj.onc.1210595.

Koundakjian, E. J., Cowan, D. M., Hardy, R. W. and Becker, A. H. (2004). The Zuker collection: a resource for the analysis of autosomal gene function in Drosophila melanogaster. *Genetics* **167**, 203-206.

Kramer, A., Mailand, N., Lukas, C., Syljuasen, R. G., Wilkinson, C. J., Nigg, E. A., Bartek, J. and Lukas, J. (2004). Centrosome-associated Chk1 prevents premature activation of cyclin-B-Cdk1 kinase. *Nat. Cell Biol.* **6**, 884-891.

Krashes, M. J., Keene, A. C., Leung, B., Armstrong, J. D. and Waddell, S. (2007). Sequential use of mushroom body neuron subsets during drosophila odor memory processing. *Neuron* **53**, 103-115.

Larocque, J. R., Jaklevic, B. R., Su, T. T. and Sekelsky, J. (2007). Drosophila ATR in double-strand break repair. *Genetics* **175**, 1023-1033.

Lee, L. A. and Orr-Weaver, T. L. (2003). Regulation of cell cycles in Drosophila development: intrinsic and extrinsic cues. *Annu. Rev. Genet.* **37**, 545-578.

Lee, L. A., Van Hoewyk, D. and Orr-Weaver, T. L. (2003). The Drosophila cell cycle kinase PAN GU forms an active complex with PLUTONIUM and GNU to regulate embryonic divisions. *Genes Dev.* **17**, 2979-2991.

Li, K. and Kaufman, T. C. (1996). The homeotic target gene centrosomin encodes an essential centrosomal component. *Cell* **85**, 585-596.

Lin, S. Y. and Elledge, S. J. (2003). Multiple tumor suppressor pathways negatively regulate telomerase. *Cell* **113**, 881-889.

Lin, S. Y., Rai, R., Li, K., Xu, Z. X. and Elledge, S. J. (2005). BRIT1/MCPH1 is a DNA damage responsive protein that regulates the Brca1-Chk1 pathway, implicating checkpoint dysfunction in microcephaly. *Proc. Natl. Acad. Sci. USA* **102**, 15105-15109.

Masrouha, N., Yang, L., Hijal, S., Larochelle, S. and Suter, B. (2003). The Drosophila chk2 gene loki is essential for embryonic DNA double-strand-break checkpoints induced in S phase or G2. *Genetics* **163**, 973-982.

Megraw, T. L., Li, K., Kao, L. R. and Kaufman, T. C. (1999). The centrosomin protein is required for centrosome assembly and function during cleavage in Drosophila. *Development* **126**, 2829-2839.

Nyberg, K. A., Michelson, R. J., Putnam, C. W. and Weinert, T. A. (2002). Toward maintaining the genome: DNA damage and replication checkpoints. *Annu. Rev. Genet.* **36**, 617-656.

O'Driscoll, M., Ruiz-Perez, V. L., Woods, C. G., Jeggo, P. A. and Goodship, J. A. (2003). A splicing mutation affecting expression of ataxia-telangiectasia and Rad3-related protein (ATR) results in Seckel syndrome. *Nat. Genet.* **33**, 497-501.

O'Farrell, P. H., Stumpff, J. and Su, T. T. (2004). Embryonic cleavage cycles: how is a mouse like a fly? *Curr. Biol.* **14**, R35-R45.

Oh, S. W., Kingsley, T., Shin, H. H., Zheng, Z., Chen, H. W., Chen, X., Wang, H., Ruan, P., Moody, M. and Hou, S. X. (2003). A P-element insertion screen identified mutations in 455 novel essential genes in Drosophila. *Genetics* **163**, 195-201.

Oikemus, S. R., McGinnis, N., Queiroz-Machado, J., Tukachinsky, H., Takada, S., Sunkel, C. E. and Brodsky, M. H. (2004). Drosophila atm/telomere fusion is required for telomeric localization of HP1 and telomere position effect. *Genes Dev.* **18**, 1850-1861.

Petermann, E. and Caldecott, K. W. (2006). Evidence that the ATR/Chk1 pathway maintains normal replication fork progression during unperturbed S phase. *Cell Cycle* **5**, 2203-2209.

Price, D., Rabinovitch, S., O'Farrell, P. H. and Campbell, S. D. (2000). Drosophila wee1 has an essential role in the nuclear divisions of early embryogenesis. *Genetics* **155**, 159-166.

Purdy, A., Uyetake, L., Cordeiro, M. G. and Su, T. T. (2005). Regulation of mitosis in response to damaged or incompletely replicated DNA require different levels of Grapes (Drosophila Chk1). *J. Cell Sci.* **118**, 3305-3315.

Raff, J. W. and Glover, D. M. (1988). Nuclear and cytoplasmic mitotic cycles continue in Drosophila embryos in which DNA synthesis is inhibited with aphidicolin. *J. Cell Biol.* **107**, 2009-2019.

Rai, R., Dai, H., Multani, A. S., Li, K., Chin, K., Gray, J., Lahad, J. P., Liang, J., Mills, G. B., Meric-Bernstam, F. et al. (2006). BRIT1 regulates early DNA damage response, chromosomal integrity, and cancer. *Cancer Cell* **10**, 145-157.

Renault, A. D., Zhang, X. H., Alphey, L. S., Frenz, L. M., Glover, D. M., Saunders, R. D. and Axton, J. M. (2003). giant nuclei is essential in the cell cycle transition from meiosis to mitosis. *Development* **130**, 2997-3005.

Rorth, P. (1998). Gal4 in the Drosophila female germline. *Mech. Dev.* **78**, 113-118.

Rothwell, W. F. and Sullivan, W. (2000). Fluorescent analysis of Drosophila embryos. In *Drosophila Protocols* (ed. W. Sullivan, M. Ashburner and R. S. Hawley), pp. 141-157. Cold Spring Harbor, NY: Cold Spring Harbor Laboratory Press.

Sibon, O. C., Stevenson, V. A. and Theurkauf, W. E. (1997). DNA-replication checkpoint control at the Drosophila midblastula transition. *Nature* **388**, 93-97.

Sibon, O. C., Laurencon, A., Hawley, R. and Theurkauf, W. E. (1999). The Drosophila ATM homologue Mei-41 has an essential checkpoint function at the midblastula transition. *Curr. Biol.* **9**, 302-312.

Sibon, O. C., Kelkar, A., Lemstra, W. and Theurkauf, W. E. (2000). DNA-replication/DNA-damage-dependent centrosome inactivation in Drosophila embryos. *Nat. Cell Biol.* **2**, 90-95.

Spradling, A. C. (1986). P-element-mediated transformation. In *Drosophila: A Practical Approach* (ed. D. B. Roberts), pp. 175-197. Oxford: IRL Press.

Stumpff, J., Duncan, T., Homola, E., Campbell, S. D. and Su, T. T. (2004). Drosophila Wee1 kinase regulates Cdk1 and mitotic entry during embryogenesis. *Curr. Biol.* **14**, 2143-2148.

Su, T. T., Campbell, S. D. and O'Farrell, P. H. (1999). Drosophila grapes/CHK1 mutants are defective in cyclin proteolysis and coordination of mitotic events. *Curr. Biol.* **9**, 919-922.

Sullivan, K. M., Scott, K., Zuker, C. S. and Rubin, G. M. (2000). The ryanodine receptor is essential for larval development in Drosophila melanogaster. *Proc. Natl. Acad. Sci. USA* **97**, 5942-5947.

Takada, S., Kelkar, A. and Theurkauf, W. E. (2003). Drosophila checkpoint kinase 2 couples centrosome function and spindle assembly to genomic integrity. *Cell* **113**, 87-99.

Takada, S., Kwak, S., Koppetsch, B. S. and Theurkauf, W. E. (2007). grp (chk1) replication-checkpoint mutations and DNA damage trigger a Chk2-dependent block at the Drosophila midblastula transition. *Development* **134**, 1737-1744.

Tang, T. T., Bickel, S. E., Young, L. M. and Orr-Weaver, T. L. (1998). Maintenance of sister-chromatid cohesion at the centromere by the Drosophila MEI-S332 protein. *Genes Dev.* **12**, 3843-3856.

Trimborn, M., Bell, S. M., Felix, C., Rashid, Y., Jafri, H., Griffiths, P. D., Neumann, L. M., Krebs, A., Reis, A., Sperling, K. et al. (2004). Mutations in microcephalin cause aberrant regulation of chromosome condensation. *Am. J. Hum. Genet.* **75**, 261-266.

Trimborn, M., Schindler, D., Neitzel, H. and Hirano, T. (2006). Misregulated chromosome condensation in MCPH1 primary microcephaly is mediated by condensin II. *Cell Cycle* **5**, 322-326.

Wakefield, J. G., Bonaccorsi, S. and Gatti, M. (2001). The drosophila protein asp is involved in microtubule organization during spindle formation and cytokinesis. *J. Cell Biol.* **153**, 637-648.

Woods, C. G., Bond, J. and Enard, W. (2005). Autosomal recessive primary microcephaly (MCPH): a review of clinical, molecular, and evolutionary findings. *Am. J. Hum. Genet.* **76**, 717-728.

Xu, J., Xin, S. and Du, W. (2001). Drosophila Chk2 is required for DNA damage-mediated cell cycle arrest and apoptosis. *FEBS Lett.* **508**, 394-398.

Xu, X., Lee, J. and Stern, D. F. (2004). Microcephalin is a DNA damage response protein involved in regulation of CHK1 and BRCA1. *J. Biol. Chem.* **279**, 34091-34094.

Yu, K. R., Saint, R. B. and Sullivan, W. (2000). The Grapes checkpoint coordinates nuclear envelope breakdown and chromosome condensation. *Nat. Cell Biol.* **2**, 609-615.

Zhong, X., Pfeifer, G. P. and Xu, X. (2006). Microcephalin encodes a centrosomal protein. *Cell Cycle* **5**, 457-458.